

## THE MULTISCALE DISCONTINUOUS GALERKIN METHOD FOR SOLVING A CLASS OF SECOND ORDER ELLIPTIC PROBLEMS WITH ROUGH COEFFICIENTS

WEI WANG, JOHNNY GUZMÁN, AND CHI-WANG SHU

**Abstract.** We develop a multiscale discontinuous Galerkin (DG) method for solving a class of second order elliptic problems with rough coefficients. The main ingredient of this method is to use a non-polynomial multiscale approximation space in the DG method to capture the multiscale solutions using coarse meshes without resolving the fine scale structure of the solution. Theoretical proofs and numerical examples are presented in both one and two dimensions. For one-dimensional problems, optimal error estimates and numerical examples are shown for arbitrary order approximations. For two-dimensional problems, numerical results are presented by the high order multiscale DG method, but the error estimate is proven only for the second order method.

**Key words.** multiscale discontinuous Galerkin method, rough coefficients

### 1. Introduction

In this paper, we consider solving a class of second order elliptic boundary value problems with highly oscillatory coefficients. Such equations arise in, e.g. composite materials and porous media. The solution oscillates rapidly and requires a very refined mesh to resolve. It is numerically difficult for traditional numerical methods to solve such problems due to the tremendous amount of computer memory and CPU time. Recently developed multiscale finite element methods [3, 13, 2, 15, 16, 11, 6, 23] provide an idea of constructing multiscale bases which are adapted to the local properties of the differential operators, allowing adequate resolution on a coarser mesh.

In particular, we are interested in the second order elliptic boundary value problems

$$(1) \quad -\nabla \cdot (A(\mathbf{x})\nabla u) = f(\mathbf{x}) \quad \text{in } \Omega$$

with the boundary condition

$$u = 0 \quad \text{on } \partial\Omega,$$

where  $\Omega$  is a rectangular domain,  $f$  is a function in  $L^2(\Omega)$  and  $A(\mathbf{x})$  is the coefficient matrix containing small scales.

In applications, Eq. (1) is the pressure equation in modeling two phase flow in porous media (see [17, 15, 6]), with  $u$  and  $A(\mathbf{x})$  interpreted as the pressure and the relative permeability tensor. Especially when the stochastic permeabilities are upscaled,  $A(\mathbf{x})$  is a diagonal tensor. Eq. (1) is also the equation of steady state heat (electrical) conduction through a composite material, with  $A(\mathbf{x})$  and  $u$  interpreted as the thermal (electric) conductivity and temperature (electric potential) (see [15]).

In the one-dimensional case,  $A(\mathbf{x}) = a(x)$  and the equation becomes

$$(2) \quad -(a(x)u_x)_x = f(x).$$

---

Received by the editors April 21, 2010.

2000 *Mathematics Subject Classification.* 65N30.

Research partially supported by NSF grant DMS-0914596, DOE grant DE-FG02-08ER25863 and NSF grant DMS-0809086.

In the two-dimensional case, we consider  $A$  with the following special form

$$A(\mathbf{x}) = \begin{pmatrix} a(x) & 0 \\ 0 & b(y) \end{pmatrix},$$

and the two-dimensional equation is

$$(3) \quad -(a(x)u_x)_x - (b(y)u_y)_y = f(x, y).$$

The typical situation in multiscale modeling, has  $a(x) = a^\varepsilon(x, \varepsilon)$  and  $b(y) = b^\varepsilon(y, \varepsilon)$  being oscillatory functions involving a small scale  $\varepsilon$ . We do not need the assumption of any periodicity of  $a^\varepsilon$  and  $b^\varepsilon$  and we do not assume any scale separation. The coefficients as well as the solution  $u$  can then have a continuum scale spectrum from  $O(\varepsilon)$  to  $O(1)$ . We only assume  $a(x)$  and  $b(y)$  belong to  $L^\infty(\Omega)$  and satisfy

$$(4) \quad 0 < \alpha \leq a(x), b(y) \leq \beta < \infty$$

for any  $(x, y) \in \Omega$ , where  $\alpha$  and  $\beta$  are constants independent of  $\varepsilon$ . If the coefficient  $a(x)$  is rough, then the solution  $u$  to (2) will also be rough; to be more specific, we will in general have

$$\|a\|_{H^1(\Omega)} \rightarrow \infty, \quad \|u\|_{H^2(\Omega)} \rightarrow \infty, \quad \text{as } \varepsilon \rightarrow 0.$$

Thus,  $u$  is not uniformly bounded with respect to  $\varepsilon$  in  $H^2(\Omega)$  or in  $H^{1+\delta}(\Omega)$  for any  $\delta > 0$ .

Notice that we are considering the special class (3) of two-dimensional problems for the convenience of explicitly constructed multiscale bases, thereby making the multiscale algorithm efficient. This special class of multiscale problems does have important applications in, e.g. two-dimensional semi-conductor quantum devices (for application of such device models in one-dimension, see [20]), in which there is a specific direction of oscillation in the coefficients at each location in space and time. We remark that the proposed numerical method can also be applied to cases with more general two-dimensional coefficients, at the price of having to numerically constructing the multiscale bases.

As early as in the 60s, Tikhonov and Samarskii [18] (see also [14]) already designed a simple 3-point finite difference scheme utilizing harmonic averages and the special solution structure of (2). In particular, the scheme in [14] can give exact solutions to the one-dimensional problem (2) at the grid points. In [3, 2], Babuška et al. proposed an approach to this kind of problems based on continuous (or non-conforming) finite element methods. In [3] theoretical proofs were provided for the one-dimensional case and arbitrary order approximation. The two-dimensional case was considered in [2], where only second-order accurate elements were considered (piecewise linear elements if  $A$  is constant). One of the difficulties in using higher order elements in multi-dimensions for the continuous Galerkin method is to make the multi-scale spaces conforming. Compared to continuous finite element methods, discontinuous Galerkin (DG) methods do not enforce continuity at the element interfaces, thus providing an easy way to construct multiscale basis in higher dimensions with high-order elements. Of course, there is a price to pay for the DG multiscale method for this flexibility: we must carefully analyze the errors associated with these discontinuities across element interfaces, to obtain high order error estimate. This is done for the arbitrary high order scheme in one dimension and for the second order scheme in two dimension in this paper. Numerical evidence indicates that our multiscale DG scheme can achieve higher than second order accuracy in two dimensions, as shown in this paper, although a proof is not available at this time.

In [23], Yuan and Shu applied the approach of Babuška et al. to the Babuška-Zlámal DG method [4]. They developed a multiscale Babuška-Zlámal DG method based on a non-polynomial basis for Eq. (2) (see [22]). Both theoretical proofs and numerical tests were presented for the one-dimensional case. Followed by Yuan and Shu's work, in [19], Wang improved the one-dimensional proof of the multiscale Babuška-Zlámal DG method by only assuming that the solution is uniformly bounded with respect to  $\varepsilon$  in  $H^1(\Omega)$ . In contrast, more regularity was assumed in [23] while proving estimates for the multiscale Babuška-Zlámal DG method.

We would like to remark that, as pointed out above, there is a three-point finite difference method developed by Tikhonov and Samarskii [18] and by Godev et al. [14], which can solve the solution of the one-dimensional problem (2) exactly at the grid points. However it seems difficult to extend this method to multi-dimensions. There are also other similar finite difference or finite volume methods such as those in [12], which are based on harmonic averages and in general have resonance errors and thus would fail in multiscale problems with no separation of scales. The methods discussed in this paper aim at obtaining uniform high order accuracy, with respect to the small scale  $\varepsilon$ , when there is no separation of scales (the problem could have a continuum of scales from  $O(\varepsilon)$  to  $O(1)$ ) and the mesh size  $h$  is much larger than  $\varepsilon$ .

In this paper we develop a multiscale symmetric interior penalty DG (IP-DG ([10, 21, 1])) method in one and two dimensions. In particular, we prove optimal error estimates in the one-dimensional case for arbitrary order approximations. We only assume that the solution is uniformly bounded with respect to  $\varepsilon$  in  $H^1(\Omega)$ . In the two-dimensional case we prove optimal error estimates for the lowest-order (second-order accurate) multiscale IP-DG method. However, we provide numerical results for higher order elements as well. Finally, we argue that the recently introduced hybridizable DG methods [8, 7] using piecewise polynomial approximations are convergent for multiscale problems considered here. However, the approximations are at most first-order accurate. This demonstrates the necessity of using multiscale non-polynomial bases when high order accuracy is desired.

## 2. Multiscale DG methods in one dimension

First we consider the one-dimensional multiscale problem (2) on the domain  $[0, 1]$  with boundary condition  $u(0) = u(1) = 0$ . Let  $I_j = (x_{j-\frac{1}{2}}, x_{j+\frac{1}{2}})$ ,  $j = 1, \dots, N$ , be a partition of  $[0, 1]$ . For simplicity, we assume that the family of partitions are quasi-uniform.

The primal formulation of the IP-DG method [10, 21, 1] is to find  $u_h \in V_h$  such that

$$(5) \quad B_h(u_h, v_h) = \int_{\Omega} f v_h dx, \quad \forall v_h \in V_h,$$

where

$$(6) \quad B_h(u, v) = \sum_{j=1}^N \int_{I_j} a u_x v_x dx - \sum_{j=0}^N ([u]_{j-1/2} \{a v_x\}_{j-1/2} + \{a u_x\}_{j-1/2} [v]_{j-1/2} + \frac{\eta}{h} [u]_{j-1/2} [v]_{j-1/2}),$$

in which  $\eta$  is a sufficiently large positive constant for maintaining stability and rates of convergence, and the average  $\{u\}$  and jump  $[u]$  are defined as follows:

$$(7) \quad [u]_{j-1/2} = u(x_{j-1/2}^+) - u(x_{j-1/2}^-), \quad \{u\}_{j-1/2} = \frac{1}{2}(u(x_{j-1/2}^+) + u(x_{j-1/2}^-)),$$

where  $u(x_{j-1/2}^+)$  and  $u(x_{j-1/2}^-)$  are the right and left limits of  $u$  at the cell boundary  $j - 1/2$ ,  $j = 1, \dots, N$ . At the domain boundaries, we have  $u(x_{1/2}^-) = 0$  and

$u(x_{N+1/2}^+) = 0$ . Here  $V_h$  is the finite element space containing functions which are discontinuous across cell interfaces. For the traditional DG methods, these functions are piecewise polynomials. For the multiscale IP-DG method, the basis functions are constructed to better approximate the solution. The multiscale basis will involve the small scales and may not be polynomials any more. The multiscale IP-DG method is constructed by using such kind of multiscale basis. We will first define the multiscale space  $V_h$  and then prove optimal error estimates for the multiscale IP-DG method.

**2.1. Multiscale space.** In our multiscale IP-DG method, the spaces are constructed below to approximate the solution to (2) (see [23, 3]):

$$(8) \quad S^k = \{\phi \in H^1(0, 1) : -(a\phi_x)_x|_{I_j} \in P^{k-2}(I_j) \text{ for each } j\}.$$

Here we define  $P^{-1}(I_j) = \{0\}$ . Hence, the multiscale IP-DG method will solve (5) with  $V_h = S^k$ .

The multiscale approximation space (8) for our model problem (2) is explicitly given by

$$(9) \quad S^k = \left\{ v : v|_{I_j} \in \text{span} \left\{ 1, \int_{x_j}^x \frac{1}{a(\xi)} d\xi, \int_{x_j}^x \frac{\xi - x_j}{a(\xi)} d\xi, \dots, \int_{x_j}^x \frac{(\xi - x_j)^{k-1}}{a(\xi)} d\xi \right\} \right\}.$$

Next, we collect some properties of the spaces  $S^k$  (see Lemma 4.1 in [3]).

*Lemma 1.* Given a function  $u \in H^1([0, 1])$ , there is a unique interpolation  $u_I \in S^k$  satisfying

$$(10) \quad \begin{aligned} u_I(x_{j+\frac{1}{2}}) &= u(x_{j+\frac{1}{2}}), \quad j = 0, 1, \dots, n, \\ \int_{I_j} (u - u_I)(x - x_{j-\frac{1}{2}})^l dx &= 0, \quad l = 0, \dots, k-2, \quad j = 1, \dots, N. \end{aligned}$$

The following approximation results hold (see Lemma 4.3 in [3]):

*Lemma 2.* Let  $u$  solve (2) and let  $u_I$  be its interpolant defined in (10), then for every  $j = 1, \dots, N$  we have

$$(11) \quad \|u - u_I\|_{L^2(I_j)} \leq C(\alpha, \beta) h^{\ell+1} \|f\|_{H^{\ell-1}(I_j)},$$

$$(12) \quad \|u - u_I\|_{H^1(I_j)} \leq C(\alpha, \beta) h^\ell \|f\|_{H^{\ell-1}(I_j)},$$

where  $C(\alpha, \beta)$  is independent of  $u$  and  $h$  but depends on  $\alpha, \beta$ . Here  $1 \leq \ell \leq k$ .

*Remark 1.* There are other ways to prove the above estimates in which one does not need to impose the continuity on the cell boundary and are able to get the same optimal approximation results as in Lemma 2, see [23].

**2.2. Error estimates.** In this section we prove optimal error estimates for the multiscale IP-DG method. For simplicity, we will consider *quasi-uniform* meshes throughout this paper. We first need to define the energy norm

$$\|v\|^2 := \sum_{j=1}^N \|\sqrt{a}v_x\|_{L^2(I_j)}^2 + h \sum_{j=0}^N \{av_x\}_{j+1/2}^2 + \frac{1}{h} [v]_{j+1/2}^2.$$

We will need the following approximation result using the energy norm.

*Lemma 3.* Let  $u$  solve (2) and let  $u_I$  be its interpolant defined in (10), then we have

$$\|u - u_I\| \leq C h^\ell \|f\|_{H^{\ell-1}([0,1])}.$$

for any  $1 \leq \ell \leq k$ .

*Proof.* Since  $u - u_I$  vanishes at all the nodes we have

$$\|u - u_I\|^2 = \sum_{j=1}^N \|\sqrt{a}(u - u_I)_x\|_{L^2(I_j)}^2 + h \sum_{j=0}^N \{a(u - u_I)_x\}_{j+1/2}^2.$$

Since  $a$  is bounded

$$\begin{aligned} \sum_{j=1}^N \|\sqrt{a}(u - u_I)_x\|_{L^2(I_j)}^2 &\leq C \|(u - u_I)_x\|_{L^2([0,1])}^2 \\ &\leq \|u - u_I\|_{H^1([0,1])}^2 \\ &\leq C h^{2\ell} \|f\|_{H^{\ell-1}([0,1])}^2. \end{aligned}$$

In the last inequality we have used (12).

To handle the other term, we use the fact that

$$\begin{aligned} &|(au_x)(x_{j-1/2}^+) - (a(u_I)_x)(x_{j-1/2}^+)| \\ &\leq |\mathbf{P}^{k-1}(au_x)(x_{j-1/2}^+) - a(u_I)_x(x_{j-1/2}^+)| + |\mathbf{P}^{k-1}(au_x)(x_{j-1/2}^+) - au_x(x_{j-1/2}^+)|, \end{aligned}$$

where  $\mathbf{P}^{k-1} : L^2(I_j) \rightarrow P^{k-1}(I_j)$  is the  $L^2$  projection onto  $P^{k-1}(I_j)$ .

If we use the trace inequality and the approximation properties of  $\mathbf{P}^{k-1}$  we have

$$\begin{aligned} &|\mathbf{P}^{k-1}(au_x)(x_{j-1/2}^+) - au_x(x_{j-1/2}^+)| \\ &\leq \frac{C}{h^{1/2}} \|\mathbf{P}^{k-1}(au_x) - au_x\|_{L^2(I_j)} + Ch^{1/2} \|(\mathbf{P}^{k-1}(au_x) - au_x)_x\|_{L^2(I_j)} \\ &\leq Ch^{\ell-1/2} \|D^\ell(au_x)\|_{L^2(I_j)} \\ &= Ch^{\ell-1/2} \|D^{\ell-1}f\|_{L^2(I_j)} \\ &\leq Ch^{\ell-1/2} \|f\|_{H^{\ell-1}(I_j)}, \end{aligned}$$

where we have used the fact that  $u$  solves the equation (2). Therefore, we have

$$h^{1/2} |(\mathbf{P}^{k-1}(au_x)(x_{j-1/2}^+) - au_x(x_{j-1/2}^+))| \leq Ch^\ell \|f\|_{H^{\ell-1}(I_j)},$$

for any  $1 \leq \ell \leq k$ . Since  $u_I \in S^k$ , we easily see that  $a(u_I)_x|_{I_j} \in P^{k-1}(I_j)$ , so by using an inverse estimate we have

$$\begin{aligned} &|\mathbf{P}^{k-1}(au_x)(x_{j-1/2}^+) - a(u_I)_x(x_{j-1/2}^+)| \\ &\leq C \frac{1}{h^{1/2}} \|\mathbf{P}^{k-1}(au_x) - a(u_I)_x\|_{L^2(I_j)} \\ &\leq C \frac{1}{h^{1/2}} \|(au_x) - a(u_I)_x\|_{L^2(I_j)} + C \frac{1}{h^{1/2}} \|\mathbf{P}^{k-1}(au_x) - au_x\|_{L^2(I_j)} \\ &\leq C \beta \frac{1}{h^{1/2}} \|u_x - (u_I)_x\|_{L^2(I_j)} + C \frac{1}{h^{1/2}} \|\mathbf{P}^{k-1}(au_x) - au_x\|_{L^2(I_j)} \\ &\leq Ch^{\ell-1/2} \|f\|_{H^{\ell-1}(I_j)}. \end{aligned}$$

In the last inequality we have used (11). Therefore,

$$h^{1/2} |(au_x)(x_{j-1/2}^+) - (a(u_I)_x)(x_{j-1/2}^+)| \leq Ch^\ell \|f\|_{H^{\ell-1}(I_j)}.$$

In a similar way we can show that

$$h^{1/2} |(au_x)(x_{j-1/2}^-) - (a(u_I)_x)(x_{j-1/2}^-)| \leq Ch^\ell \|f\|_{H^{\ell-1}(I_{j-1})}.$$

Using this result and adding the contribution of every node we get

$$h \sum_{j=0}^N \{a(u - u_I)_x\}_{j+1/2}^2 \leq Ch^{2\ell} \|f\|_{H^{\ell-1}([0,1])}^2.$$

Hence,

$$\| \| u - u_I \| \|^2 \leq C h^{2\ell} \| f \|_{H^{\ell-1}([0,1])}^2.$$

The result now follows after we take the square root on both sides.  $\square$

Now we can state our main result of this section.

*Theorem 2.1.* Let  $u_h \in V_h = S^k$  be the multiscale IP-DG solution of (5), then we have

$$(13a) \quad \| \| u - u_h \| \leq C h^k \| f \|_{H^{k-1}([0,1])}$$

$$(13b) \quad \| u - u_h \|_{L^2([0,1])} \leq C h^{k+1} \| f \|_{H^{k-1}([0,1])}.$$

*Proof.* We first prove (13a). To do this we collect some results about the bilinear form  $B_h(\cdot, \cdot)$  defined in (6). The first result follows easily by applying the Cauchy-Schwartz inequality and using the fact that  $a$  is bounded.

*Lemma 4.* (Boundedness) There exists a constant  $C_b$  such that

$$B_h(w, v) \leq C_b \| \| w \| \| \| v \| \quad \forall w, v \in V_h = S^k.$$

The second result concerns the coercivity of the bilinear form.

*Lemma 5.* (Stability) There exists some constant  $C_s$  such that

$$(14) \quad B_h(v, v) \geq C_s \| \| v \| \|^2 \quad \forall v \in V_h = S^k.$$

The proof of this lemma, when  $V_h$  is the space of piecewise polynomials, is contained in [1] (in the multi-dimensional case as well). The case when  $V_h = S^k$  is similar, with the main difference being that we have to apply an inverse estimate to functions of the form  $av_x$ . However, by the definition of  $S^k$  we have  $av_x|_{I_j} \in P^{k-1}(I_j)$  hence we can apply inverse estimates; see the proof of the two-dimensional case in the next section for a similar idea.

Finally, using integration by parts we can easily prove the following Galerkin orthogonality result.

*Lemma 6.* (Orthogonality) We have the following orthogonality equality

$$B_h(u - u_h, v) = 0 \quad \forall v \in V_h = S^k.$$

Using Lemmas 5, 6 and 4 we obtain

$$C_s \| \| u_I - u_h \| \|^2 \leq B_h(u_I - u, u_I - u_h) \leq C_b \| \| u - u_I \| \| \| u_I - u_h \| \|.$$

Hence,

$$\| \| u_I - u_h \| \leq \frac{C_b}{C_s} \| \| u - u_I \| \|.$$

Therefore, the triangle inequality gives

$$\| \| u - u_h \| \leq \left( 1 + \frac{C_b}{C_s} \right) \| \| u - u_I \| \|.$$

The inequality (13a) now follows from Lemma 3.

In order to prove (13b), we define the dual problem

$$(15) \quad -(a\varphi_x)_x = u - u_h, \quad [0, 1],$$

with the boundary conditions

$$(16) \quad \varphi(0) = \varphi(1) = 0.$$

Therefore,

$$\begin{aligned} \|u - u_h\|_{L^2([0,1])}^2 &= - \int_0^1 (u - u_h) (a\varphi_x)_x dx \\ &= B_h(u - u_h, \varphi). \end{aligned}$$

In the last equation we used the consistency and symmetry of the IP-DG bilinear form  $B_h(\cdot, \cdot)$ .

Using Lemma 6 we get

$$\|u - u_h\|_{L^2([0,1])}^2 = B_h(u - u_h, \varphi - \varphi_I),$$

where  $\varphi_I$  is the interpolant of  $\varphi$  defined in (10). By Lemma 4 we get

$$\|u - u_h\|_{L^2([0,1])}^2 \leq C_b \| \|u - u_h\| \| \varphi - \varphi_I \| \|.$$

By using Lemma 3 (with  $\ell = 1$ ) we have  $\| \varphi - \varphi_I \| \leq Ch \|u - u_h\|_{L^2([0,1])}$ . We arrive at

$$\|u - u_h\|_{L^2([0,1])} \leq Ch \| \|u - u_h\| \|.$$

The inequality (13b) now follows from (13a).  $\square$

### 3. Multiscale DG methods in two dimensions

We now consider the two-dimensional elliptic multiscale problem (3) on a square domain  $[-1, 1]^2$ . Let  $\mathcal{T}_h$  be a collection of *quasi-uniform rectangular* partitions of  $\Omega$  and  $\mathcal{E}_h$  be the collection of edges of the  $\mathcal{T}_h$ . Define the following inner products

$$\begin{aligned} (v, w)_{\mathcal{T}_h} &= \sum_{K \in \mathcal{T}_h} \int_K v(x, y) \cdot w(x, y) dx dy, \\ \langle v, w \rangle_{\mathcal{E}_h} &= \sum_{e \in \mathcal{E}_h} \int_e v(s) \cdot w(s) ds. \end{aligned}$$

The IP method finds  $u_h \in V_h$  such that

$$(17) \quad B_h(u_h, v_h) = (f, v_h)_{\mathcal{T}_h} \quad \forall v_h \in V_h,$$

where the bilinear form is defined by

$$B_h(u, v) := (A\nabla u, \nabla v)_{\mathcal{T}_h} - \langle \{A\nabla u\}, [v] \rangle_{\mathcal{E}_h} - \langle \{A\nabla v\}, [u] \rangle_{\mathcal{E}_h} + \frac{\eta}{h} \langle [u], [v] \rangle_{\mathcal{E}_h}$$

and  $\eta$  is a sufficiently large positive constant. For a scalar valued function  $u$ , we define the average  $\{u\}$  and the jump  $[u]$  as follows. Let  $e$  be an interior edge shared by elements  $K_1$  and  $K_2$ . Define the unit normal vectors  $\mathbf{n}_1$  and  $\mathbf{n}_2$  on  $e$  pointing exterior to  $K_1$  and  $K_2$ , respectively. With  $u_i := u|_{\partial K_i}$ , we set

$$(18) \quad \{u\} = \frac{1}{2}(u_1 + u_2), \quad [u] = u_1 \mathbf{n}_1 + u_2 \mathbf{n}_2 \quad \text{on } e \in \mathcal{E}_h^o,$$

where  $\mathcal{E}_h^o$  is the set of interior edges  $e$ . For a vector-valued function  $\mathbf{q}$  we define  $\mathbf{q}_1$  and  $\mathbf{q}_2$  analogously and set

$$(19) \quad \{\mathbf{q}\} = \frac{1}{2}(\mathbf{q}_1 + \mathbf{q}_2), \quad [\mathbf{q}] = \mathbf{q}_1 \cdot \mathbf{n}_1 + \mathbf{q}_2 \cdot \mathbf{n}_2 \quad \text{on } e \in \mathcal{E}_h^o.$$

For  $e \in \mathcal{E}_h^\partial$ , the set of boundary edges, we set

$$(20) \quad [u] = u\mathbf{n}, \quad \{\mathbf{q}\} = \mathbf{q} \quad \text{on } e \in \mathcal{E}_h^\partial,$$

where  $\mathbf{n}$  is the outward unit normal. We do not require either of the quantities  $\{u\}$  or  $[\mathbf{q}]$  on boundary edges, and we leave them undefined.

In this section, the high order multiscale IP-DG method for the two dimensional case will be constructed, however the optimal error estimate will be shown only for the second order method.

**3.1. Multiscale spaces.** The one-dimensional approach can be easily expanded to the two-dimensional case, i.e. we construct the two-dimensional multiscale approximation space as follows (see [23]):

$$(21) \quad S_2^k = \{\phi \in H^1(\Omega) : -(a(x)\phi_x)_x - (b(y)\phi_y)_y|_K \in P^{k-2}(K), \text{ for all } K \in \mathcal{T}_h\},$$

where  $(x_K, y_K)$  is the barycenter of the element  $K$ . In particular,

$$S_2^1 = \left\{ v : v|_K \in \text{span} \left\{ 1, \int_{x_K}^x \frac{1}{a(\xi)} d\xi, \int_{y_K}^y \frac{1}{b(\eta)} d\eta, \right\} \right\},$$

$$S_2^2 = \left\{ v : v|_K \in \text{span} \left\{ 1, \int_{x_K}^x \frac{1}{a(\xi)} d\xi, \int_{y_K}^y \frac{1}{b(\eta)} d\eta, \int_{x_K}^x \frac{\xi - x_K}{a(\xi)} d\xi, \int_{x_K}^x \frac{1}{a(\xi)} d\xi \int_{y_K}^y \frac{1}{b(\eta)} d\eta, \int_{y_K}^y \frac{\eta - y_K}{b(\eta)} d\eta \right\} \right\}.$$

For higher  $k$  it is more difficult to find an explicit formula for the multiscale basis (21).

**3.2. Error estimates.** Here we give an error analysis of the lowest-order ( $k = 1$ ) IP-DG method. In order to do so, we define the following energy norm

$$\|v\|^2 := (A\nabla v, \nabla v)_{\mathcal{T}_h} + \frac{1}{h} \langle \llbracket v \rrbracket, \llbracket v \rrbracket \rangle_{\mathcal{E}_h} + h \langle \{\!\{ A\nabla v \}\!\}, \{\!\{ A\nabla v \}\!\} \rangle_{\mathcal{E}_h}.$$

We now state our main result.

*Theorem 3.1.* Let  $u$  be the solution of (3) and let  $u_h \in V_h = S_2^1$  be the IP-DG approximation, then

$$(22a) \quad \|u - u_h\| \leq C h \|f\|_{L^2(\Omega)},$$

$$(22b) \quad \|u - u_h\|_{L^2(\Omega)} \leq C h^2 \|f\|_{L^2(\Omega)}.$$

Before we prove this theorem we will state and prove some important lemmas.

*Lemma 7.* The following stability result holds

$$\|v\|^2 \leq C B_h(v, v) \quad \forall v \in V_h = S_2^1.$$

*Proof.* Let  $v \in V_h$ , then by the definition of  $B_h(\cdot, \cdot)$  we get

$$(23) \quad B_h(v, v) = (A\nabla v, \nabla v)_{\mathcal{T}_h} - 2 \langle \{\!\{ A\nabla v \}\!\}, \llbracket v \rrbracket \rangle_{\mathcal{E}_h} + \frac{\eta}{h} \langle \llbracket v \rrbracket, \llbracket v \rrbracket \rangle_{\mathcal{E}_h}.$$

By the arithmetic-geometric mean inequality we get that

$$(24) \quad 2 \langle \{\!\{ A\nabla v \}\!\}, \llbracket v \rrbracket \rangle_{\mathcal{E}_h} \leq \frac{1}{\delta h} \langle \llbracket v \rrbracket, \llbracket v \rrbracket \rangle_{\mathcal{E}_h} + h \delta \langle \{\!\{ A\nabla v \}\!\}, \{\!\{ A\nabla v \}\!\} \rangle_{\mathcal{E}_h},$$

for any  $\delta > 0$ . Next, we bound  $h \delta \langle \{\!\{ A\nabla v \}\!\}, \{\!\{ A\nabla v \}\!\} \rangle_{\mathcal{E}_h}$ . One can easily show that

$$(25) \quad \langle \{\!\{ A\nabla v \}\!\}, \{\!\{ A\nabla v \}\!\} \rangle_{\mathcal{E}_h} \leq 2 \sum_{K \in \mathcal{T}_h} \int_{\partial K} (A\nabla v) \cdot (A\nabla v).$$

By the definition of  $V_h$ ,  $A\nabla v \in P^1(K)$  on each triangle  $K \in \mathcal{T}_h$ . Hence, by a standard inverse inequality for the space  $P^1(K)$

$$\int_{\partial K} (A\nabla v) \cdot (A\nabla v) \leq C_{\text{inv}} h^{-1} \int_K (A\nabla v) \cdot (A\nabla v) \leq C_{\text{inv}} \beta h^{-1} \int_K (A\nabla v) \cdot \nabla v.$$

Hence,

$$(26) \quad h\delta \langle \{\{A\nabla v\}\}, \{\{A\nabla v\}\} \rangle_{\mathcal{E}_h} \leq 2\delta C_{\text{inv}\beta}(A\nabla v, \nabla v)_{\mathcal{T}_h}.$$

If we plug this result into (24) we get

$$(27) \quad 2\langle \{\{A\nabla v\}\}, \llbracket v \rrbracket \rangle_{\mathcal{E}_h} \leq \frac{1}{\delta h} \langle \llbracket v \rrbracket, \llbracket v \rrbracket \rangle_{\mathcal{E}_h} + 2\delta C_{\text{inv}\beta}(A\nabla v, \nabla v)_{\mathcal{T}_h}.$$

Using (23) we obtain

$$\begin{aligned} B_h(v, v) &\geq (A\nabla v, \nabla v)_{\mathcal{T}_h} + \frac{\eta}{h} \langle \llbracket v \rrbracket, \llbracket v \rrbracket \rangle_{\mathcal{E}_h} - \frac{1}{\delta h} \langle \llbracket v \rrbracket, \llbracket v \rrbracket \rangle_{\mathcal{E}_h} \\ &\quad - 2\delta C_{\text{inv}\beta}(A\nabla v, \nabla v)_{\mathcal{T}_h} \\ &= (1 - 2\delta C_{\text{inv}\beta})(A\nabla v, \nabla v)_{\mathcal{T}_h} + \left(\frac{\eta}{h} - \frac{1}{\delta h}\right) \langle \llbracket v \rrbracket, \llbracket v \rrbracket \rangle_{\mathcal{E}_h}. \end{aligned}$$

If we choose  $\delta$  so that  $(1 - 2\delta C_{\text{inv}\beta}) \leq \frac{1}{2}$  and if we assume that  $\eta$  is sufficiently large so that  $\eta \geq \frac{1}{2\delta}$ , then we get

$$(A\nabla v, \nabla v)_{\mathcal{T}_h} + \frac{1}{h} \langle \llbracket v \rrbracket, \llbracket v \rrbracket \rangle_{\mathcal{E}_h} \leq C B(v, v).$$

Finally, the proof is complete if we use (26).  $\square$

The next lemma concerns approximation properties of the space  $S_2^1$ .

*Lemma 8.* Let  $u$  solve (3). Then, there exists  $v \in V_h = S_2^1$  so that

$$\|u - v\| \leq Ch \|f\|_{L^2(\Omega)}.$$

*Proof.* We start with a natural transformation. Define

$$\begin{aligned} \hat{x} &:= \int_{-1}^x \frac{1}{a(s)} ds \\ \hat{y} &:= \int_{-1}^y \frac{1}{b(s)} ds. \end{aligned}$$

We see that the transformation  $(x, y) \rightarrow (\hat{x}, \hat{y})$  maps  $\Omega = [-1, 1] \times [-1, 1]$  to  $\hat{\Omega} = [-1, \int_{-1}^1 \frac{1}{a(s)} ds] \times [-1, \int_{-1}^1 \frac{1}{b(s)} ds]$ . Also it maps the rectangle  $K \in \mathcal{T}_h$  to a rectangle  $\hat{K}$ .

Accordingly, for any function  $u$  defined on  $\Omega$  we define a function  $\hat{u}$  on  $\hat{\Omega}$  by

$$\hat{u}(\hat{x}, \hat{y}) := u(x, y).$$

Define  $\hat{v}$  to be the piece-wise linear function defined on  $\hat{\Omega}$  such that  $\hat{v}|_{\hat{K}} \in P^1(\hat{K})$  satisfies

$$h_{\hat{K}} \|\nabla(\hat{u} - \hat{v})\|_{L^2(\hat{K})} + \|\hat{u} - \hat{v}\|_{L^2(\hat{K})} \leq Ch_{\hat{K}}^2 |D^2 \hat{u}|_{L^2(\hat{K})},$$

where  $h_{\hat{K}} = \text{diam}(\hat{K})$ .

Now define  $v \in L^2(\Omega)$ , such that on each  $K \in \mathcal{T}_h$

$$v(x, y) := \hat{v}(\hat{x}, \hat{y}).$$

We easily see that  $v \in V_h$ .

It is clear that

$$\|u - v\|_{L^2(K)} \leq \frac{1}{\alpha} \|\hat{u} - \hat{v}\|_{L^2(\hat{K})} \leq Ch_{\hat{K}}^2 |D^2 \hat{u}|_{L^2(\hat{K})}.$$

Taking the sum over  $K \in \mathcal{T}_h$  we get

$$(28) \quad \|u - v\|_{L^2(\Omega)} \leq Ch^2 |D^2 \hat{u}|_{L^2(\hat{\Omega})},$$

where we have used that  $h_{\hat{K}} \leq Ch_K$ .

We also obtain

$$\begin{aligned}
 \int_K A\nabla(u-v) \cdot \nabla(u-v) dx dy &\leq \frac{1}{\alpha} \int_K A\nabla(u-v) \cdot A\nabla(u-v) dx dy \\
 &= \frac{1}{\alpha} \int_{\hat{K}} \nabla(\hat{u}-\hat{v}) \cdot \nabla(\hat{u}-\hat{v}) \hat{a}(\hat{x}) \hat{b}(\hat{y}) d\hat{x} d\hat{y} \\
 &\leq \frac{\beta^2}{\alpha} \int_{\hat{K}} \nabla(\hat{u}-\hat{v}) \cdot \nabla(\hat{u}-\hat{v}) d\hat{x} d\hat{y} \\
 &\leq Ch_K^2 |D^2 \hat{u}|_{L^2(\hat{K})}^2.
 \end{aligned}$$

Hence, if we sum over  $K$  we get that

$$(29) \quad (A\nabla(u-v), \nabla(u-v))_{\mathcal{T}_h} \leq Ch^2 |D^2 \hat{u}|_{L^2(\hat{\Omega})}^2.$$

Finally, we set that

$$\begin{aligned}
 &\int_K \nabla(A\nabla(u)) : \nabla(A\nabla(u)) dx dy \\
 &= \int_{\hat{K}} \left( \frac{1}{\hat{a}} \partial_{\hat{x}}^2 \hat{u} + \left( \frac{1}{\hat{a}} + \frac{1}{\hat{b}} \right) \partial_{\hat{x}} \partial_{\hat{y}} \hat{u} + \frac{1}{\hat{b}} \partial_{\hat{y}}^2 \hat{u} \right) \hat{a} \hat{b} d\hat{x} d\hat{y} \\
 &\leq \frac{\beta^2}{\alpha} |D^2 \hat{u}|_{L^2(\hat{K})}^2.
 \end{aligned}$$

Hence,

$$(30) \quad \sum_{K \in \mathcal{T}_h} \|\nabla(A\nabla u)\|_{L^2(K)}^2 \leq C |D^2 \hat{u}|_{L^2(\hat{\Omega})}^2.$$

From the definition of  $\|\cdot\|$  we see that

$$\begin{aligned}
 \|u-v\|^2 &= (A\nabla(u-v), \nabla(u-v))_{\mathcal{T}_h} + \frac{1}{h} \langle \llbracket (u-v) \rrbracket, \llbracket (u-v) \rrbracket \rangle_{\mathcal{E}_h} \\
 &\quad + h \langle \{\!\{ A\nabla(u-v) \}\!\}, \{\!\{ A\nabla(u-v) \}\!\} \rangle_{\mathcal{E}_h}.
 \end{aligned}$$

We bound each term individually. The first term was bounded in (29). For the second term we use a trace inequality to get

$$\begin{aligned}
 \frac{1}{h} \langle \llbracket (u-v) \rrbracket, \llbracket (u-v) \rrbracket \rangle_{\mathcal{E}_h} &\leq \frac{C}{h^2} \|u-v\|_{L^2(\Omega)}^2 + C \|\nabla(u-v)\|_{L^2(\Omega)}^2 \\
 &\leq \frac{C}{h^2} \|u-v\|_{L^2(\Omega)}^2 + C \frac{1}{\alpha} (A\nabla(u-v), \nabla(u-v))_{\mathcal{T}_h} \\
 &\leq Ch^2 |D^2 \hat{u}|_{L^2(\hat{\Omega})}^2.
 \end{aligned}$$

In the last inequality we used (28) and (29).

If we use a trace inequality we get that

$$\begin{aligned}
 &h \langle \{\!\{ A\nabla(u-v) \}\!\}, \{\!\{ A\nabla(u-v) \}\!\} \rangle_{\mathcal{E}_h} \\
 &\leq C \sum_{K \in \Omega_h} \|A\nabla(u-v)\|_{L^2(K)}^2 + Ch^2 \sum_{K \in \mathcal{T}_h} \|\nabla(A\nabla u)\|_{L^2(K)}^2 \\
 &\leq \frac{C}{\alpha} (A\nabla(u-v), \nabla(u-v))_{\mathcal{T}_h} + Ch^2 \sum_{K \in \mathcal{T}_h} \|\nabla(A\nabla u)\|_{L^2(K)}^2 \\
 &\leq Ch^2 |D^2 \hat{u}|_{L^2(\hat{\Omega})}^2,
 \end{aligned}$$

where we have used (29) and (30). We ave also used the fact that  $\nabla(A\nabla v)|_K = 0$  for  $v \in V_h$  and  $K \in \mathcal{T}_h$ .

Hence,

$$\|u - v\|^2 \leq Ch^2 |D^2 \hat{u}|_{L^2(\hat{\Omega})}^2.$$

In order to complete the proof we argue that

$$(31) \quad |D^2 \hat{u}|_{L^2(\hat{\Omega})} \leq C \|f\|_{L^2(\Omega)}.$$

We easily see that

$$\begin{aligned} -\frac{1}{\hat{a}} \partial_{\hat{x}}^2 \hat{u} - \frac{1}{\hat{b}} \partial_{\hat{y}}^2 \hat{u} &= \hat{f} & \hat{\Omega}, \\ \hat{u} &= 0, & \partial \hat{\Omega}. \end{aligned}$$

By Bernstein's Theorem [5] we get that

$$|D^2 \hat{u}|_{L^2(\hat{\Omega})} \leq C \|\hat{f}\|_{L^2(\hat{\Omega})}.$$

Finally, using the fact that  $\|\hat{f}\|_{L^2(\hat{\Omega})} \leq C \|f\|_{L^2(\Omega)}$  gives (31) and this completes the proof.  $\square$

We can now prove Theorem 3.1.

*Proof.* We first prove (22a). To this end, by Lemma 7 we have

$$\|v - u_h\|^2 \leq C B_h(v - u_h, v - u_h),$$

for any  $v \in V_h$ .

By the Galerkin orthogonality of the IP-DG method we have

$$\|v - u_h\|^2 \leq C B_h(v - u, v - u_h).$$

Clearly,  $B_h(\cdot, \cdot)$  is a bounded bilinear form. That is,

$$B_h(v - u, v - u_h) \leq C \|v - u\| \|v - u_h\|.$$

Therefore,

$$\|v - u_h\| \leq C \|v - u\|.$$

The triangle inequality gives

$$\|u - u_h\| \leq C \|v - u\|.$$

Since this holds for any  $v \in V_h$ , Lemma 8 gives (22a).

In order to prove (22b), we will use a duality argument. We define the problem

$$(32a) \quad -(a(x)\phi_x(x, y))_x - (b(y)\phi_y(x, y))_y = (u - u_h)(x, y), \quad (x, y) \in \Omega = [-1, 1]^2,$$

$$(32b) \quad \phi(x, y) = 0, \quad (x, y) \in \partial\Omega.$$

By the adjoint consistency of the IP-DG method we have

$$\|u - u_h\|_{L^2(\Omega)}^2 = B_h(u - u_h, \phi) = B_h(u - u_h, \phi - v),$$

for any  $v \in V_h$ . Here we have used the Galerkin orthogonality. Hence,

$$\|u - u_h\|_{L^2(\Omega)}^2 \leq C \|u - u_h\| \|\phi - v\| \leq Ch \|u - u_h\| \|u - u_h\|_{L^2(\Omega)},$$

where we have used Lemma 8. The inequality (22b) now follows after we apply (22a).  $\square$

#### 4. Numerical results

In this section, both one- and two-dimensional examples are presented to demonstrate that the proposed multiscale IP-DG method can capture the small scales in a very coarse mesh whereas the traditional IP-DG method (i.e. that uses piecewise polynomial spaces) cannot do that. We will use the notation  $q = \nabla u$  and  $q_h = \nabla u_h$  in the error tables.

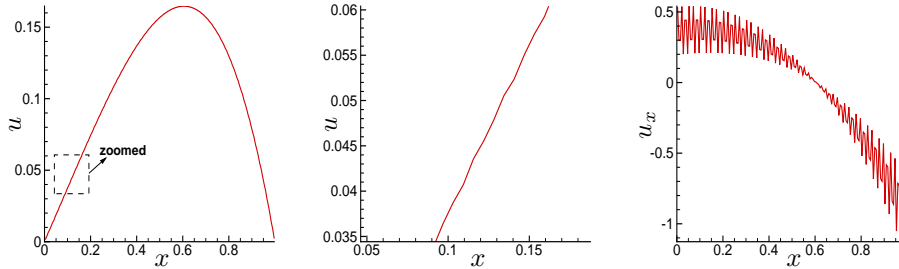


FIGURE 1. Exact solution of the one-dimensional example 1. Left:  $u$ ; middle: zoomed part of  $u$ ; right:  $u_x$ .

**4.1. One-dimensional examples.** The first one-dimensional example is the same as that in [23]. However the results are computed by the proposed multiscale IP-DG method. The second example is used to show  $a(x) = a^\varepsilon(x, \varepsilon)$  does not have separation of scales. In both cases, the multi-scale IP-DG method shows the optimal order of convergence for the solution with a very small  $\varepsilon = 0.01$  and  $\varepsilon = 0.001$  starting from coarse meshes. The stabilization parameter in the IP-DG method is taken as  $\eta = 10$ .

**4.1.1. One-dimensional example 1.** Consider the one-dimensional multiscale problem Eq. (2) with

$$(33) \quad a(x) = a^\varepsilon(x, \varepsilon) = \frac{1}{2 + x + \sin\left(\frac{2\pi x}{\varepsilon}\right)}, \quad f = x, \quad x \in [0, 1].$$

The exact solution of Eq. (33) with  $\varepsilon = 0.01$  is plotted in Fig. 1. The solution itself is oscillatory in the level of  $\varepsilon$ . However the derivative of the solution is oscillating rapidly (see Fig. 1 right).

We first run this multiscale problem by the traditional IP-DG method with polynomial basis. Table 1 shows the  $L^2$  errors and orders of accuracy for  $\varepsilon = 0.01$  and  $\varepsilon = 0.001$ . We can see that, for  $\varepsilon = 0.01$ , the traditional IP-DG method starts to converge from the mesh size  $N = 320$ . However, for  $\varepsilon = 0.001$ , we cannot see any order of convergence even when the mesh is refined to  $N = 640$ . This is because the traditional IP-DG method can only have the expected order of convergence when the mesh is refined enough relative to  $\varepsilon$ , which is consistent with the error estimates for such DG method based on regular piecewise polynomials. We remark that high order traditional IP-DG methods will have the same phenomenon, which we do not show here.

Next we test our multiscale IP-DG method for this multiscale problem with both  $\varepsilon = 0.01$  and  $\varepsilon = 0.001$ . The numerical results are shown in Table 2. We can clearly see the expected order of accuracy which is  $(k + 1)$ th order for  $u$  and  $k$ th order for  $q$  for the multiscale IP-DG method, starting from very coarse meshes.

**4.1.2. One-dimensional example 2.** In the second example, the coefficient  $a^\varepsilon$  is not periodic in  $x$  or  $\frac{x}{\varepsilon}$  and there is no clear scale separation. Consider the multiscale problem with

$$(34) \quad a^\varepsilon(x, \varepsilon) = \frac{1}{2 + x + \sin\left(\frac{\sin x}{\varepsilon} \cos x\right)}, \quad f = -\cos x, \quad x \in [0, 1].$$

TABLE 1.  $L^2$  errors and orders of accuracy by the traditional IP-DG method with polynomial basis  $P^1$ : one-dimensional example 1.

N	$\varepsilon = 0.01$				$\varepsilon = 0.001$			
	$u - u_h$		$q - q_h$		$u - u_h$		$q - q_h$	
	error	order	error	order	error	order	error	order
10	1.02E-02	–	1.20E-01	–	1.05E-02	–	6.06E-02	–
20	9.82E-03	0.05	1.12E-01	0.10	9.97E-03	0.08	1.56E-01	-1.36
40	9.60E-03	0.03	1.10E-01	0.02	9.89E-03	0.01	1.12E-01	0.48
80	8.85E-03	0.12	1.09E-01	0.01	9.89E-03	0.00	1.12E-01	0.00
160	6.33E-03	0.48	9.67E-02	0.17	8.95E-03	0.14	1.11E-01	0.01
320	2.50E-03	1.34	5.73E-02	0.75	8.99E-03	-0.01	1.11E-01	0.00
640	7.45E-04	1.75	2.98E-02	0.94	8.56E-03	0.07	1.08E-01	0.04

TABLE 2.  $L^2$  errors and orders of accuracy by the multiscale IP-DG method: one-dimensional example 1.

$S^1$	$\varepsilon = 0.01$				$\varepsilon = 0.001$			
	$u - u_h$		$q - q_h$		$u - u_h$		$q - q_h$	
	error	order	error	order	error	order	error	order
N	1.03E-03	–	4.73E-02	–	1.03E-03	–	4.74E-02	–
10	2.61E-04	1.98	2.36E-02	1.00	2.62E-04	1.97	2.37E-02	1.00
20	6.71E-05	1.96	1.18E-02	1.00	6.62E-05	1.98	1.19E-02	1.00
40	1.68E-05	2.00	5.86E-03	1.01	1.67E-05	1.99	5.93E-03	1.01
80	3.89E-06	2.11	2.80E-03	1.06	4.17E-06	2.00	2.96E-03	1.00
$S^2$	$u - u_h$		$q - q_h$		$u - u_h$		$q - q_h$	
N	error	order	error	order	error	order	error	order
10	1.16E-05	–	1.01E-03	–	1.15E-05	–	1.01E-03	–
20	1.48E-06	2.97	2.48E-04	2.03	1.46E-06	2.98	2.52E-04	2.00
40	1.89E-07	2.97	6.14E-05	2.01	1.83E-07	2.99	6.28E-05	2.00
80	2.29E-08	3.04	1.51E-05	2.03	2.30E-08	2.99	1.57E-05	2.00
160	2.84E-09	3.01	3.74E-06	2.01	2.94E-09	2.97	3.94E-06	1.99

We perform numerical tests by the multiscale IP-DG method on Eq. (34) with  $\varepsilon = 0.01$  and  $\varepsilon = 0.001$ . Table 3 shows the  $L^2$  errors and orders of accuracy. We can again clearly see the expected order of accuracy which is  $(k + 1)$ th order for  $u$  and  $k$ th order for  $q$ , starting from very coarse meshes.

**4.2. Two-dimensional example.** We now consider three two-dimensional elliptic multiscale examples on the domain  $[-1, 1]^2$ . The first example is made up from the one-dimensional example thus has the exact solution. The second and third examples are real two-dimensional examples which do not have explicit formulas for their exact solutions. Thus we compute reference solutions by a spectral Chebyshev collocation method with a mesh  $512 \times 512$  in order to check the convergence rates of the DG methods.

We remark that in the second and third examples, due to the difficulties of computing a very refined reference solution, we are unable to test a very small  $\varepsilon$  (we tested  $\varepsilon = 0.01$  and  $\varepsilon = 0.005$ ). The smaller the  $\varepsilon$  is, the bigger the advantage

TABLE 3.  $L^2$  errors and orders of accuracy by the multiscale IP-DG method: one-dimensional example 2.

		$\varepsilon = 0.01$				$\varepsilon = 0.001$			
<hr/>									
$S^1$		$u - u_h$		$q - q_h$		$u - u_h$		$q - q_h$	
N		error	order	error	order	error	order	error	order
10		1.50E-03	-	6.36E-02	-	1.44E-03	-	6.18E-02	-
20		3.51E-04	2.09	2.92E-02	1.12	3.67E-04	1.97	3.09E-02	1.00
40		8.95E-05	1.97	1.50E-02	0.96	9.26E-05	1.99	1.54E-02	1.00
80		2.33E-05	1.94	7.68E-03	0.97	2.33E-05	1.99	7.61E-03	1.02
160		5.93E-06	1.97	3.87E-03	0.99	5.55E-06	2.07	3.59E-03	1.08
<hr/>									
$S^2$		$u - u_h$		$q - q_h$		$u - u_h$		$q - q_h$	
N		error	order	error	order	error	order	error	order
10		8.39E-06	-	5.74E-04	-	7.87E-06	-	5.60E-04	-
20		1.10E-06	2.94	1.38E-04	2.05	9.75E-07	3.01	1.40E-04	2.00
40		1.41E-07	2.97	3.50E-05	1.98	1.27E-07	2.94	3.49E-05	2.00
80		1.77E-08	3.00	8.80E-06	1.99	1.59E-08	2.99	8.51E-06	2.04
160		2.21E-09	3.00	2.20E-06	2.00	1.96E-09	3.02	2.14E-06	1.99

of the multiscale IP-DG method we should see. This is because the error of the multiscale IP-DG method does not depend on  $\varepsilon$ , but the traditional IP-DG method can only have convergence when the mesh size is small enough to resolve the  $\varepsilon$  scale.

**4.3. Two-dimensional example 1.** The first two-dimensional example is the Eq. (3) with

$$(35) \quad a(x) = a^\varepsilon(x, \varepsilon) = \frac{1}{4 + x + \sin\left(\frac{x}{\varepsilon}\right)}, \quad b(y) = b^\varepsilon(y, \varepsilon) = \frac{1}{4 + y + \sin\left(\frac{y}{\varepsilon}\right)}.$$

In order to construct a two-dimensional example with an exact solution, we make up the solution from the one-dimensional example. The solution has the form  $u(x, y) = u^e(x)u^e(y)$ , where  $u^e(x)$  is the exact solution of the one-dimensional problem  $-(a(x)u_x)_x = f_1$  with  $a(x)$  in (35) (note that  $b(x) = a(x)$ ) and  $f_1 = x$ . The right-hand-side  $f(x, y)$  in Eq. (3) is then

$$(36) \quad f(x, y) = xu^e(y) + yu^e(x).$$

Note that the right-hand-side  $f(x, y)$  contains the  $O(\varepsilon)$  scale, however its  $H^1$ -norm is uniformly bounded, so our theory would apply, at least up to second order accuracy.

Table 4 lists the  $L^2$  errors and orders of convergence of the multiscale IP-DG method for  $\varepsilon = 0.01$  and  $\varepsilon = 0.001$ . We can see the optimal convergences for both  $u$  and  $q$  with the  $S_2^1$  and  $S_2^2$  spaces, starting from very coarse meshes (recall that our proof of optimal convergence is only for  $S_2^1$ ).

**4.4. Two-dimensional example 2.** In the second example, we consider a smooth function of  $f(x, y)$  with the same coefficients  $a(x)$  and  $b(y)$  in Eq. (35), i.e.,

$$(37) \quad a(x) = a^\varepsilon(x, \varepsilon) = \frac{1}{4 + x + \sin\left(\frac{x}{\varepsilon}\right)},$$

$$b(y) = b^\varepsilon(y, \varepsilon) = \frac{1}{4 + y + \sin\left(\frac{y}{\varepsilon}\right)}, \quad f = x + y.$$

For this example, an explicit formula for the exact solution is unavailable, and we are using the numerically obtained reference solution. We only list the  $L^2$  errors and orders of  $u$  of the multiscale IP-DG method (see Table 5). We can see an almost

TABLE 4.  $L^2$  errors and orders of accuracy by the multiscale IP-DG method: two-dimensional example 1.

$\varepsilon = 0.01$					$\varepsilon = 0.001$				
$S_2^1$	$u - u_h$		$q - q_h$		$u - u_h$		$q - q_h$		
N	error	order	error	order	error	order	error	order	
10	1.41E-02	–	2.79E-02	–	1.39E-02	–	2.80E-02	–	
20	4.79E-03	1.56	1.30E-02	1.11	4.87E-03	1.52	1.30E-02	1.11	
40	1.36E-03	1.82	6.08E-03	1.10	1.40E-03	1.80	6.07E-03	1.10	
80	3.57E-04	1.93	2.95E-03	1.04	3.69E-04	1.92	2.94E-03	1.05	
$S_2^2$	$u - u_h$		$q - q_h$		$u - u_h$		$q - q_h$		
N	error	order	error	order	error	order	error	order	
10	3.91E-04	–	3.79E-03	–	3.90E-04	–	3.79E-03	–	
20	4.63E-05	3.08	9.45E-04	2.00	4.59E-05	3.09	9.40E-04	2.01	
40	5.53E-06	3.07	2.35E-04	2.00	5.60E-06	3.04	2.34E-04	2.01	
80	7.03E-07	2.98	5.88E-05	2.00	6.96E-07	3.01	5.82E-05	2.01	

second order convergence for the multiscale IP-DG method with the  $S_2^1$  space and an almost third order convergence with  $S_2^2$ , starting from very coarse meshes. This shows the optimal convergence rates of the multiscale IP-DG method. Compared to the multiscale IP-DG results, the  $L^2$  errors and orders by the traditional IP-DG method with polynomial spaces  $P^1$  and  $P^2$  are listed in Table 6. For the relative large  $\varepsilon = 0.01$ , we can see the convergence of the traditional IP-DG method from the mesh size  $N = 80$ . When  $\varepsilon$  goes smaller to 0.005, we cannot see a correct order of convergence especially in the  $P^2$  case for the meshes we have tested.

TABLE 5.  $L^2$  errors and orders of accuracy by the multiscale IP-DG method: two-dimensional example 2.

$\varepsilon = 0.01$				$\varepsilon = 0.005$	
$S_2^1$					
N	error	order	error	order	
10	4.16E-02	–	4.04E-02	–	
20	1.28E-02	1.71	1.31E-02	1.63	
40	3.56E-03	1.85	3.59E-03	1.87	
80	9.42E-04	1.92	9.50E-04	1.92	
$S_2^2$					
10	1.25E-03	–	1.25E-03	–	
20	1.82E-04	2.78	1.85E-04	2.75	
40	2.54E-05	2.84	2.59E-05	2.84	
80	3.57E-06	2.83	3.56E-06	2.86	

**4.5. Two-dimensional example 3.** In the third example, the coefficients  $a^\varepsilon$  and  $b^\varepsilon$  do not have separation of scales:

$$(38) \quad \begin{aligned} a(x) &= a^\varepsilon(x, \varepsilon) = \frac{1}{4+x+\sin\left(\frac{\sin x}{\varepsilon} \cos x\right)}, \\ b(y) &= b^\varepsilon(y, \varepsilon) = \frac{1}{4+y+\sin\left(\frac{\sin y}{\varepsilon} \cos y\right)}, \quad f = x + y. \end{aligned}$$

TABLE 6.  $L^2$  errors and orders of accuracy by traditional IP-DG method with polynomial basis  $P^1$ : two-dimensional example 2.

	$\varepsilon = 0.01$		$\varepsilon = 0.005$	
$P^1$				
10	4.98E-02	–	4.97E-02	–
20	2.22E-02	1.16	2.33E-02	1.10
40	1.37E-02	0.69	1.39E-02	0.75
80	5.33E-03	1.36	1.11E-02	0.32
$P^2$				
10	1.06E-02	–	1.16E-02	–
20	1.09E-02	-0.04	1.06E-02	0.13
40	5.14E-03	1.08	1.08E-02	-0.02
80	7.49E-04	2.78	5.06E-03	1.09

Again, an explicit formula for the exact solution is unavailable, and we are using the numerically obtained reference solution.

We perform numerical tests by the multiscale IP-DG method on Eq. (3) with (38) for  $\varepsilon = 0.01$  and  $\varepsilon = 0.005$ . Table 7 shows the  $L^2$  errors and orders of accuracy. We can again clearly see the expected order of accuracy which is  $(k + 1)$ th order for  $u$ , starting from very coarse meshes.

TABLE 7.  $L^2$  errors and orders of accuracy by the multiscale IP-DG method: two-dimensional example 3.

	$\varepsilon = 0.01$		$\varepsilon = 0.005$	
$S_2^1$				
N	error	order	error	order
10	4.00E-02	–	6.45E-02	–
20	1.26E-02	1.67	1.80E-02	1.84
40	3.54E-03	1.83	4.83E-03	1.90
80	9.34E-04	1.92	1.22E-03	1.98
$S_2^2$				
10	1.23E-03	–	1.34E-03	–
20	1.81E-04	2.76	1.84E-04	2.87
40	2.64E-05	2.78	2.57E-05	2.84
80	3.69E-06	2.84	3.55E-06	2.85

## 5. DG methods with polynomial basis for multiscale problems

In this section, we are going to show that some DG methods with piecewise constant approximations can approximate the multiscale problem (2) and (3) with first-order accuracy. However, if higher-order accuracy is required then one needs to use multiscale basis in the previous sections. We include this section because this is one of the few numerical methods, based on piecewise polynomials, which can yield convergence (albeit with a low first-order accuracy) when the mesh size is too coarse to resolve the  $\varepsilon$ -scale.

Falk and Osborn [13] argued that some mixed methods can approximate rough solutions of the problem (3) using piecewise polynomial approximations. Here we

argue that the single face-hybridizable (SF-H) method [7] can also approximate rough solutions to (3) using piecewise polynomial approximations. Hybridizable-DG (HDG) methods were recently introduced in [8]. The SF-H [7] method is a special class of HDG methods where on each triangle one only penalizes on exactly one edge. The minimal dissipation local DG (MD-LDG) method [7] is a limiting case of the HDG methods where the penalization parameter is allowed to be infinite (see [8] for more details). We will first give the error estimates for the HDG methods. Then we will show the numerical results by the limiting case MD-LDG method.

**5.1. Error estimates for the hybridizable DG methods.** In order to define the SF-H method for (3), we need to rewrite (3) in its mixed form. We let

$$(39) \quad A^{-1} \mathbf{q} + \nabla u = 0$$

$$(40) \quad \nabla \cdot \mathbf{q} = f$$

where  $A$  is given by

$$A(\mathbf{x}) = \begin{pmatrix} a(x) & 0 \\ 0 & b(y) \end{pmatrix}.$$

We let  $\{\mathcal{T}_h\}$  be a collection of shape-regular *triangular* partitions of  $\Omega$ . Let  $\mathcal{E}_h$  be the collection of edges of  $\mathcal{T}_h$ . We define the function spaces corresponding the lowest-order SF-H method

$$(41a) \quad \boldsymbol{\Sigma}_h = \{\mathbf{v} \in [L^2(\Omega)]^2 : \mathbf{v}|_K \in [P^0(K)]^2 \forall K \in \mathcal{T}_h\},$$

$$(41b) \quad W_h = \{w \in L^2(\Omega) : w|_K \in P^0(K) \forall K \in \mathcal{T}_h\},$$

$$(41c) \quad M_h = \{\mu \in L^2(\mathcal{E}_h) : \mu|_e \in P^0(e) \forall e \in \mathcal{E}_h, \text{ and } \mu = 0 \text{ on } \partial\Omega\}.$$

The approximation  $(\mathbf{q}_h, u_h, \lambda_h) \in \boldsymbol{\Sigma}_h \times W_h \times M_h$  is determined by requiring that

$$(42a) \quad (A^{-1} \mathbf{q}_h, \mathbf{v})_{\mathcal{T}_h} - (u_h, \nabla \cdot \mathbf{v})_{\mathcal{T}_h} + \langle \lambda_h, \mathbf{v} \cdot \mathbf{n} \rangle_{\partial\mathcal{T}_h} = 0,$$

$$(42b) \quad -(\mathbf{q}_h, \nabla \omega)_{\mathcal{T}_h} + \langle \hat{\mathbf{q}}_h \cdot \mathbf{n}, \omega \rangle_{\partial\mathcal{T}_h} = (f, \omega)_{\partial\mathcal{T}_h},$$

$$(42c) \quad \langle \hat{\mathbf{q}}_h \cdot \mathbf{n}, \mu \rangle_{\partial\mathcal{T}_h} = 0,$$

for all  $(\mathbf{v}, \omega, \mu) \in \boldsymbol{\Sigma}_h \times W_h \times M_h$ , where

$$(42d) \quad \hat{\mathbf{q}}_h := \mathbf{q}_h + \tau(u_h - \lambda_h) \mathbf{n} \quad \text{on } \partial K \text{ for all } K \in \mathcal{T}_h.$$

Here  $\mathbf{n}$  is the outward pointing unit normal to an element  $K \in \mathcal{T}_h$ . Moreover, we used the following notation

$$\langle \mathbf{v} \cdot \mathbf{n}, \mu \rangle_{\partial\mathcal{T}_h} := \sum_{K \in \mathcal{T}_h} \int_{\partial K} \mathbf{v}(\gamma) \cdot \mathbf{n} \mu(\gamma) d\gamma.$$

The penalty parameters  $\tau$  is a double-valued constant function on each interior edge of the triangulation  $\mathcal{T}_h$ . The SF-H method chooses  $\tau|_K$  so that it is zero on all but one edge of  $\partial K$ . More precisely, it chooses an arbitrary edge  $e_K^r$  of  $\partial K$ . Then it sets  $\tau = \tau_K > 0$  on  $e_K^r$  but it sets  $\tau = 0$  on  $\partial K \setminus e_K^r$ . With such a choice one has the property that  $\mathbf{q}_h$  and  $\lambda_h$  are independent of  $\tau$ ; see [7]. However,  $u_h$  will depend on  $\tau$ . We note that  $\lambda_h$  is the so-called Lagrange multiplier that approximates  $u$  on the edges of the triangulation  $\mathcal{T}_h$ . In fact, one can locally eliminate  $\mathbf{q}_h, u_h$  to get a final system for  $\lambda_h$ , then one can recover  $\mathbf{q}_h, u_h$  element-by-element; see [7, 8].

We now state the main result of this section.

*Theorem 5.1.* Let  $u$  solve (3) and let  $(\mathbf{q}_h, u_h, \lambda_h) \in \Sigma_h \times W_h \times M_h$  solve (42), then

$$(43) \quad \|\nabla u + A^{-1}\mathbf{q}_h\|_{L^2(\Omega)} \leq Ch\|f\|_{L^2(\Omega)}.$$

Moreover, if  $\tau_K \geq \frac{c}{h_K}$  for some constant  $c > 0$  and all  $K \in \mathcal{T}_h$ , then

$$(44) \quad \|u - u_h\|_{L^2(\Omega)} \leq Ch\|f\|_{L^2(\Omega)}.$$

*Proof.* By Theorem 2.5 in [7] we have

$$\|A^{-1/2}(\mathbf{q} - \mathbf{q}_h)\|_{L^2(\Omega)} = Ch\|\mathbf{q}\|_{H^1(\Omega)}.$$

Hence,

$$\begin{aligned} \|\nabla u + A^{-1}\mathbf{q}_h\|_{L^2(\Omega)} &\leq \|A^{-1}(-\mathbf{q} + \mathbf{q}_h)\|_{L^2(\Omega)} \\ &\leq \frac{1}{\alpha} \|A^{-1/2}(-\mathbf{q} + \mathbf{q}_h)\|_{L^2(\Omega)} \\ &\leq Ch\|\mathbf{q}\|_{H^1(\Omega)}. \end{aligned}$$

Using Bernstein's regularity result [5], Falk and Osborn [13] proved that  $A\nabla u \in H^1(\Omega)$  uniformly although  $u$  may not belong to  $H^2(\Omega)$  uniformly. In fact, they proved

$$\|A\nabla u\|_{H^1(\Omega)} \leq C\|f\|_{L^2(\Omega)}.$$

Since  $\mathbf{q} = -A\nabla u$  we have proven (43).

In order to prove (44) we use Corollary 2.7 in [7] that gives

$$\|u - u_h\|_{L^2(\Omega)} \leq Ch(\|\mathbf{q}\|_{H^1(\Omega)} + \|u\|_{H^1(\Omega)}).$$

Here we have used our hypothesis  $\tau_K \geq \frac{c}{h_K}$  for some constant  $c > 0$  and all  $K \in \mathcal{T}_h$ .

We already argued that  $\|\mathbf{q}\|_{H^1(\Omega)} \leq \|f\|_{L^2(\Omega)}$ . Clearly, by an energy argument we have  $\|u\|_{H^1(\Omega)} \leq \|f\|_{L^2(\Omega)}$ . This proves (44).  $\square$

A few comments are in order. First, it is no surprise that the SF-H method is convergent for (3) since the SF-H method is very similar to the standard mixed methods. Also, more general HDG methods (e.g. allowing  $\tau = 1$  everywhere) are convergent for (3); however, one needs to trace the effects of the penalty parameters  $\tau$  on the error  $\mathbf{q} - \mathbf{q}_h$ ; see [9]. Finally, we point out that higher-order SF-H methods would not give better results since  $\mathbf{q} \in H^1(\Omega)$  but not uniformly in  $H^2(\Omega)$ .

**5.2. Numerical tests by MD-LDG.** If we formally set  $\tau^- = 0$  and  $\tau^+ = \infty$  on all the interior edges of the triangulation  $\mathcal{T}_h$ , then the HDG method will result in the MD-LDG method (see [8]).

Table 8 shows the numerical results by the piecewise constant MD-LDG method for the one-dimensional multiscale problem example 1 (33). We can see a clear first order convergence for both  $u$  and the derivative of  $u$ .

We remark that higher order MD-LDG schemes can give the optimal convergence for the derivative of  $u$  but not for  $u$ , because the function  $au_x$  does not involve the small scale and thus the polynomial basis can well approximate  $\mathbf{q}$  in the implementation for Eq. (39). In other words, if MD-LDG is implemented in the following way

$$(45) \quad \mathbf{q} + \nabla u = 0$$

$$(46) \quad \nabla \cdot A\mathbf{q} = f,$$

we will not be able to see convergence before the small scale is resolved. We do not include these numerical results here.

The numerical results for the two-dimensional multiscale problem example 2 (37) are listed in Table 9 for  $\varepsilon = 0.01$  and  $\varepsilon = 0.005$ . We can see that the piecewise constant MD-LDG method also shows a first order convergence in the two-dimensional case.

TABLE 8.  $L^2$  errors and orders of accuracy by the MD-LDG with polynomial basis  $P^0$ : one-dimensional example 1.

N	$\varepsilon = 0.01$				$\varepsilon = 0.001$			
	$u - u_h$		$\mathbf{q} - \mathbf{q}_h$		$u - u_h$		$\mathbf{q} - \mathbf{q}_h$	
	error	order	error	order	error	order	error	order
10	2.21E-02	–	2.69E-02	–	2.23E-02	–	2.69E-02	–
20	1.16E-02	0.93	1.24E-02	1.12	1.18E-02	0.92	1.24E-02	1.12
40	6.01E-03	0.95	5.90E-03	1.07	5.99E-03	0.98	5.88E-03	1.08
80	3.03E-03	0.99	2.86E-03	1.04	3.02E-03	0.99	2.86E-03	1.04
160	1.53E-03	0.98	1.41E-03	1.02	1.51E-03	1.00	1.41E-03	1.03

TABLE 9.  $L^2$  errors and orders of accuracy by the MD-LDG method with polynomial basis  $P^0$ : two-dimensional example 2.

N	$\varepsilon = 0.01$		$\varepsilon = 0.005$	
	error	order	error	order
10	4.14E-01	–	4.16E-01	–
20	2.16E-01	0.94	2.18E-01	0.93
40	1.09E-01	0.99	1.10E-01	0.99
80	5.50E-02	0.99	5.45E-02	1.01
160	2.74E-02	1.01	2.73E-02	1.00

## 6. Concluding remarks

In this paper, we developed a multiscale IP-DG method for solving a class of second order elliptic equations with rough coefficients in one and two dimensions. Assuming that the solution lies only uniformly in  $H^1$  with respect to the small  $\varepsilon$  scale, we prove optimal error estimates for arbitrary order approximations for the one dimensional case and optimal error estimates for the second order approximation for the two-dimensional case for coarse meshes which do not resolve the small  $\varepsilon$  scale. Numerical tests are performed in both one and two dimensions, demonstrating high order accuracy by the multiscale IP-DG method on coarse meshes. In addition, the proof of first order convergence of the HDG method with polynomial basis is given and related numerical test is shown for the MD-LDG method. In future work, we plan to generalize the analysis and develop multiscale DG methods for various elliptic problems.

## References

- [1] D. N. Arnold, *An interior penalty finite element method with discontinuous elements*, SIAM J. Numer. Anal., **39**, 1982, 742–760.
- [2] I. Babuška, G. Caloz and J. Osborn, *Special finite element methods for a class of second order elliptic problems with rough coefficients*, SIAM J. Numer. Anal., **31**, 1994, 945–981.
- [3] I. Babuška and J. Osborn, *Generalized finite element methods: their performance and their relation to mixed methods*, SIAM J. Numer. Anal., **20**, 1983, 510–536.

- [4] I. Babuška and M. Zlámal, *Nonconforming elements in the finite element method with penalty*, SIAM J. Numer. Anal., **10**, 1973, 863–875.
- [5] S.N. Bernstein, *Sur la généralisation du problème de Dirichlet*, Math. Ann., **62**, 1906, 253–271.
- [6] Z. Chen and T.Y. Hou, *A mixed multiscale finite element method for elliptic problems with oscillating coefficients*, Math. Comp., **72**, 2002, 541–576.
- [7] B. Cockburn, B. Dong and J. Guzmán, *A superconvergent LDG-hybridizable Galerkin method for second-order elliptic problems*, Math. Comp., **77**, 2008, 1887–1916.
- [8] B. Cockburn, J. Gopalakrishnan and R. Lazarov, *Unified hybridization of discontinuous Galerkin, mixed, and continuous Galerkin methods for second order elliptic problems*, SIAM J. Numer. Anal., **47**, 2009, 1319–1365.
- [9] B. Cockburn, J. Guzmán and H. Wang, *Superconvergent discontinuous Galerkin methods for second-order elliptic problems*, Math. Comp., **78**, 2009, 1–24.
- [10] J. Douglas Jr. and T. Dupont, *Interior Penalty Procedures for Elliptic and Parabolic Galerkin Methods*, Lecture Notes in Phys. 58, Springer-Verlag, Berlin, 1976.
- [11] Y.R. Efendiev, T.Y. Hou and X.H. Wu, *The convergence of nonconforming multiscale finite element methods*, SIAM J. Numer. Anal., **37**, 2000, 888–910.
- [12] R. Ewing, O. Iliev and R. Lazarov, *A modified finite volume approximation of second-order elliptic equations with discontinuous coefficients*, SIAM J. Sci. Comput., **23**, 2001, 1335–1351.
- [13] R.S. Falk and J.E. Osborn, *Remarks on mixed finite element methods for problems with rough coefficient*, Math. Comp., **62**, 1994, 1–19.
- [14] K.N. Godev, R.D. Lazarov, V.L. Makarov and A.A. Samarskii, *Homogeneous difference schemes for one-dimensional problems with generalized solutions*, Math USSR SB, **59**, 1988, 155–179.
- [15] T.Y. Hou and X.H. Wu, *A multiscale finite element method for elliptic problems in composite materials and porous media*, J. Comput. Phys., **134**, 1997, 169–189.
- [16] T.Y. Hou, X.H. Wu and Z. Cai, *Convergence of a multiscale finite element method for elliptic problems with rapidly oscillating coefficients*, Math. Comp., **68**, 1999, 913–943.
- [17] P. Langlo and M.S. Espedal, *Macrodispersion for two-phase, immiscible flow in porous media*, Adv. in Water Resources, **17**, 1994, 297–316.
- [18] A.N. Tikhonov and A.A. Samarskii, *Homogeneous difference schemes*, USSR Computational Mathematics and Mathematical Physics, **1**, 1962, 5–67.
- [19] W. Wang, *Multiscale discontinuous Galerkin methods and applications*, Ph.D. Thesis, Brown University, 2008.
- [20] W. Wang and C.-W. Shu, *The WKB local discontinuous Galerkin method for the simulation of Schrödinger equation in a resonant tunneling diode*, J. Sci. Comput., **40**, 2009, 360–374.
- [21] M.F. Wheeler, *An elliptic collocation-finite element method with interior penalties*, SIAM J. Numer. Anal., **15**, 1978, 152–161.
- [22] L. Yuan and C.-W. Shu, *Discontinuous Galerkin method based on non-polynomial approximation spaces*, J. Comput. Phys., **218**, 2006, 295–323.
- [23] L. Yuan and C.-W. Shu, *Discontinuous Galerkin method for a class of elliptic multi-scale problems*, Int. J. Numer. Meth. Fluids, **56**, 2008, 1017–1032.

Center for Turbulence Research, Stanford University, Stanford, CA 94305  
*E-mail*: [weiwang1@stanford.edu](mailto:weiwang1@stanford.edu).

Division of Applied Mathematics, Brown University, Providence, RI 02912  
*E-mail*: [jguzman@dam.brown.edu](mailto:jguzman@dam.brown.edu)  
*E-mail*: [shu@dam.brown.edu](mailto:shu@dam.brown.edu)